Acoustic scattering by a cylinder near a pressure release surface

Zhen Ye and You-Yu Chen
Department of Physics, National Central University, Chungli, Taiwan 32054, Republic of China

(April 3, 2001)

Abstract

This paper presents a study of acoustic scattering by a cylinder of either infinite or finite length near a flat pressure-release surface. A novel self-consistent method is developed to describe the multiple scattering interactions between the cylinder and the surface. The complete scattering amplitude for the cylinder is derived from a set of equations, and is numerically evaluated. The results show that the presence of the surface can either enhance or reduce the scattering of the cylinder, depending on the frequency, the composition of the cylinder, and the distance between the cylinder and the surface. Both air-filled and rigid cylinders are considered.

PACS number: 43.30.Gv., 43.30.Bp., 43.20.Fn.

INTRODUCTION

Acoustic scattering by underwater objects near a pressure release boundary is a very important issue in a number of current research and applications, including the modeling of scattering from surface dwelling fish, the understanding of oceanic fluxes and ambient noises generated at ocean surface layers. It may also be of great help in models of acoustic scattering by submarines near the ocean surface.

In the literature, the research on sound scattering by underwater objects near a pressure release surface has been mainly focused on the scattering by a spherical object such as an air bubble (Refs. e. g. [1, 2, 3, 4, 5, 6, 7]). In many important applications, however, underwater objects may not take the spherical geometry. Rather they often take elongated shapes. This includes, for example, the surface dwelling fish, the floating logs in rivers, military objects, and so on. For these situations, it is desirable to study acoustic scattering by an elongated object near a boundary. By searching the literature, we find that the research along this line is surprisingly scarce. The purpose of the the present paper is to present an investigation of acoustic scattering by a cylinder of either infinite or finite length near a flat pressure-release boundary.

We consider acoustic scattering by an elongated object near a flat pressure release surface; the sea or river surface can be regarded as one of such surfaces when the acoustic wavelength is long compared to the surface wave. As a first step, for simplicity yet not to compromising the generality, we assume the object as a straight cylinder. Due to the presence of the surface, the wave will be scattered back and forth between the surface and the object before it reaches a receiver. The rescattering from the scatterer and rereflection from the surface are studied using a self-consistent method by expressing all the waves in terms of modal series. The scattering by the cylinder is thus exactly evaluated, and analyzed. The theory is first developed for an infinite cylinder, then extended to finite cylinders using the genuine approach given by Ref. [8]. Although the theory allows us to consider a variety of cylinders, in order to show the essence of the theory in its most transparent way we focus on two important types of cylinders, that is, the air-filled and the rigid cylinders. The former can be used to model the fish while the latter may resemble some acoustic scattering characteristics of military objects.

I. FORMULATION OF THE PROBLEM

The problem considered in this paper is depicted in Fig. 1. A straight cylinder is located in the water at a depth d beneath a pressure release plane which can be the sea surface. For simplicity, we assume that the axis of the cylinder is parallel to the plane. The radius of the cylinder is a. The acoustic parameters of the cylinder are taken as: the mass density ρ_1 and sound speed c_1, while those of the surround water are ρ and c; therefore the acoustic contrasts are $g = \rho_1/\rho$ and $h = c_1/c$. A parallel line acoustic source transmitting a wave of frequency ω is at $\vec{r}_s$ some distance away from the surface. The transmitted wave is scattered by

the cylinder and reflected from the surface, as shown in Fig. 1. The reflected wave is also scattered by the cylinder. The wave scattered by the cylinder is again reflected by the surface. Such a process is repeated, establishing an infinite series of rescattering and rereflection between the cylinder and the surface. This multiple scattering process can be conveniently treated by a self-consistent manner. The rectangular frame is set up in such a way that the z-axis is parallel to the axis of the cylinder. the x-axis and y-axis are shown in Fig. 1. To solve the scattering problem, however, we use the cylindrical coordinates in the rectangular system. We note that in the present paper, for brevity we do not consider the case that the incident direction is oblique to the axis of the cylinder; the extension to oblique cases is straightforward. The setting in the problem is by analogy with that described in Ref. [7], where a spherical air bubble is placed beneath the flat boundary.

A. Scattering by a cylinder of infinite length

In this section, we present a formulation for sound scattering by an infinite cylinder near a pressure-release boundary. For succinctness, we only show the most essential steps in the derivation. First the direct wave from the line source can be written as

$$p_{inc} = i\pi H_0^{(1)}(k|\vec{r} - \vec{r}_s|), \tag{1}$$

with k being the wave number of the transmitted wave ($k = \omega/c$), and $H_0^{(1)}$ being the zero-th order Hankel function of the first kind. The reason why we choose to use the line source is that it can easily used to include the usual plane wave situation; for this we just need to put the source at a place so that $k|\vec{r} - \vec{r}_s| >> 1$. Due to the presence of the pressure release surface, the reflection from the surface of the direct wave can be regarded as coming from an image source located symmetrically about the surface, and is written as

$$p_r = -i\pi H_0^{(1)}(k|\vec{r} - \vec{r}_{si}|), \tag{2}$$

where $\vec{r}_{si}$ is the vector coordinate for the image, which is at the parity position about the plane.

The scattered wave from the cylinder can be generally written as

$$p_{s1} = \sum_{n=-\infty}^{\infty} A_n H_n^{(1)}(k|\vec{r} - \vec{r}_1|)e^{in\phi_{\vec{r}-\vec{r}_1}}, \tag{3}$$

where A_n are the coefficients to be determined later, $H_n^{(1)}$ are the n-th order Hankel functions of the first kind, and ϕ is the azimuthal angle that sweeps through the plane perpendicular to the longitudinal axis of the cylinder. According to Brekhovskikh[9], the effect of the boundary on the cylinder can be represented by introducing an image cylinder located at the mirror symmetry site about the plane surface. The rereflection and rescattering between the surface and the cylinder can be represented by the multiple scattering between the cylinder and its image. The scattered wave from this image can be similarly written as

$$p_{s2} = \sum_{n=-\infty}^{\infty} B_n H_n^{(1)}(k|\vec{r} - \vec{r}_2|)e^{in\phi_{\vec{r}-\vec{r}_2}}, \tag{4}$$

where $\vec{r}_2$ is the location of the image of the cylinder, which is symmetric about the pressure-release plane. At the pressure release surface, the boundary condition requires $p_{s1} + p_{s2} = 0$, leading to

$$B_n = -A_{-n}, \tag{5}$$

where we have used the relations

$$\phi_{\vec{r}-\vec{r}_1} = \pi - \phi_{\vec{r}-\vec{r}_2}, \quad \text{and} \quad H_n^{(1)}(x) = (-1)^n H_{-n}^{(1)}(x).$$

Similarly the wave inside the cylinder can be written as

$$p_{in} = \sum_{n=-\infty}^{\infty} C_n J_n(k|\vec{r} - \vec{r}_1|)e^{in\phi_{\vec{r}-\vec{r}_1}}. \tag{6}$$

Again, C_n are the unknown coefficients, and J_n are the n-th order Bessel functions of the first kind.

To solve for the unknown coefficients A_n (thus B_n) and C_n, we employ the boundary conditions at the surface of the cylinder. For the purpose, we express all wave fields in the coordinates with respect to the position of the cylinder. This can be achieved by using the addition theorem for the Hankel functions

$$H_n^{(1)}(k|\vec{r}-\vec{r}'|)e^{in\phi_{\vec{r}-\vec{r}'}} = e^{in\phi_{\vec{r}_1-\vec{r}'}} \sum_{l=-\infty}^{\infty} H_{n-l}^{(1)}(k|\vec{r}_1-\vec{r}'|)e^{-il\phi_{\vec{r}_1-\vec{r}'}} J_l(k|\vec{r}-\vec{r}_1|)e^{il\phi_{\vec{r}-\vec{r}_1}}, \tag{7}$$

where $\vec{r}'$ can either be the location of the source by setting $\vec{r}' = \vec{r}_s$, the location of the image of the source with $\vec{r}' = \vec{r}_{si}$, or the location of the image of the cylinder with $\vec{r}' = \vec{r}_2$. The boundary conditions on the surface of the cylinder state that both the acoustic field and the radial displacement be continuous across the interface. Applying the addition theorem to the expressions for the concerned waves in Eqs. (1), (2), (4), and (6), then plugging them into the boundary conditions, and after a careful calculation, we are led to the following equation

$$D_l - \sum_{n=-\infty}^{\infty} A_{-n} e^{i(n-l)\phi_{\vec{r}_1-\vec{r}_2}} H_{n-l}^{(1)}(k|\vec{r}_1-\vec{r}_2|) = \Gamma_l A_l, \tag{8}$$

where we have used

$$B_n = -A_{-n}.$$

In Eq. (8), we derived

$$\Gamma_l = -\frac{H_l^{(1)}(ka)J_l'(ka/h) - ghH_l^{(1)'}(ka)J_l(ka/h)}{J_l(ka)J_l'(ka/h) - ghJ_l'(ka)J_l(ka/h)}, \tag{9}$$

and

$$D_l = i\pi \left[H_{-l}^{(1)}(k|\vec{r}_1-\vec{r}_s|)e^{-il\phi_{\vec{r}_1-\vec{r}_s}} - H_{-l}^{(1)}(k|\vec{r}_1-\vec{r}_{si}|)e^{-il\phi_{\vec{r}_1-\vec{r}_{si}}} \right]. \tag{10}$$

The coefficients A_n are thus determined by a set of self-consistent equations in (8). Once A_n are found, the total scattered wave can be evaluated from

$$\begin{aligned} p_s &= p_{s1} + p_{s2} \\ &= \sum_{n=-\infty}^{\infty} \left[A_n H_n^{(1)}(k|\vec{r}-\vec{r}_1|)e^{in\phi_{\vec{r}-\vec{r}_1}} + B_n H_n^{(1)}(k|\vec{r}-\vec{r}_2|)e^{in\phi_{\vec{r}-\vec{r}_2}} \right]. \end{aligned} \tag{11}$$

In the far field limit, $r \to \infty$, by expanding the Hankel functions, we have

$$\begin{aligned} p_s &\approx \sqrt{\frac{2}{\pi r}} e^{ikr} \sum_{n=-\infty}^{\infty} e^{-i(n\pi/2+\pi/4)} \left[A_n e^{-ik\vec{r}_1\cdot\hat{r}} + B_n e^{-ik\vec{r}_2\cdot\hat{r}} \right] e^{in\phi_{\vec{r}}} \\ &= \sqrt{\frac{2}{\pi r}} Q e^{ikr}, \end{aligned} \tag{12}$$

where we define

$$Q \equiv \sum_{n=-\infty}^{\infty} e^{-i(n\pi/2+\pi/4)} \left[A_n e^{-ik\vec{r}_1\cdot\hat{r}} + B_n e^{-ik\vec{r}_2\cdot\hat{r}} \right] e^{in\phi_{\vec{r}}}, \tag{13}$$

with $B_n = -A_{-n}$, as a measure of the scattering strength.

B. Scattering by a cylinder of finite length

In practice, we are often concerned with acoustic scattering by objects of finite length. Here we consider the scattering by a finite cylinder beneath a flat pressure release surface such as the sea plane. The problem of acoustic scattering by a finite object has been difficult enough, let alone the presence of a boundary. Exact solutions only exist for simply shaped objects. Approximate methods have been developed. A review on various methods for computing sound scattering by an isolated elongated object is presented in Ref. [8]. In this section, we extend the cylinder-method proposed in Ref. [8], devised for an isolated cylinder, to the present case of a cylinder near a boundary. The reason for choosing this method is that it has been verified both theoretically and experimentally that this method is reasonably accurate for a wide range of situations[10, 11]. This is particularly true for the scenarios discussed in the present paper.

From the Kirchhoff integral theorem, the scattering function from any scatter can be evaluated from

$$f(\vec{r},\vec{r}_i) = -\frac{e^{-ik\vec{r}_1\cdot\hat{r}}}{4\pi} \int_S ds' e^{-ik\vec{r}'\cdot\hat{r}} \vec{n}\cdot\left[\nabla_{r'} p_s(\vec{r}') + ik\hat{r}p_s(\vec{r}')\right], \tag{14}$$

where $\vec{n}$ is an outwardly directed unit vector normal to the surface, and $\hat{r}$ is the unit vector in the scattering direction defined as $\hat{r} = \vec{r}/r$. Function $f(\vec{r}, \vec{r}_i)$ refers to the scattering function for incident direction at $\vec{r}_i$ implicit in the scattering field $p_s(\vec{r})$ and the scattering direction $\hat{r}$.

First we consider the scattering from the cylinder. Then in Eq. (14), the field p_s is the scattering field taking values at the surface of scatterer. According to [8], this can be mimicked by that of an infinite cylinder of the same radius. On the surface of the cylinder (not the image), from Eq. (3) the scattered field can be expressed as

$$p_{s1} = \sum_{n=-\infty}^{\infty} A_n H_n^{(1)}(ka) e^{in\phi}, \tag{15}$$

and

$$\vec{n} \cdot \nabla_{r'} p_{s1} = \sum_{n=-\infty}^{\infty} A_n k H_n^{(1)'}(ka) e^{in\phi}. \tag{16}$$

Then the integral for the scattering function of the cylinder, using Eq. (14), becomes

$$f^c(\vec{r}, \vec{r}_i) = \sum_{n=-\infty}^{\infty} f_n(\vec{r}, \vec{r}_i), \tag{17}$$

with

$$\begin{aligned} f_n(\vec{r}, \vec{r}_i) &= \frac{-aLA_n e^{-ik\vec{r}_1 \cdot \hat{r}}}{4\pi} \int_0^{2\pi} d\phi e^{-ika\cos(\phi_{scat} - \phi)} \\ &\quad \times \left[ik\cos(\phi_{scat} - \phi) H_n^{(1)}(ka) e^{in\phi} + k H_n^{(1)'}(ka) e^{in\phi} \right], \end{aligned} \tag{18}$$

where ϕ_{scat} is the scattering angle with respect to $x-$axis (i. e. $\phi_{scat} = \phi_{\vec{r}}$).

Using integral identities

$$\int_0^{2\pi} d\phi e^{-ika\cos(\phi - \phi_{scat})} e^{in\phi} = 2\pi(-i)^n J_n(ka) e^{in\phi_{scat}}, \tag{19}$$

and

$$\int_0^{2\pi} d\phi e^{-ika\cos(\phi - \phi_{scat})} \cos(\phi - \phi_{scat}) e^{in\phi} = 2\pi(-i)^n i J_n'(ka) e^{in\phi_{scat}}, \tag{20}$$

we can reduce Eq. (18) to

$$f_n(\vec{r}, \vec{r}_i) = \frac{-kaL(-i)^n A_n e^{-ik\vec{r}_1 \cdot \hat{r}}}{2} e^{in\phi_{scat}} \left[H_n^{(1)}(ka)' J_n(ka) - H_n^{(1)}(ka) J_n'(ka) \right]. \tag{21}$$

By the Wronskian identity

$$[J_n(x) H_n^{(1)'}(x) - J_n'(x) H_n^{(1)}(x)] = \frac{2i}{\pi x}, \tag{22}$$

Eq. (21) becomes

$$f_n(\vec{r}, \vec{r}_i) = \frac{-i(-i)^n L A_n e^{-ik\vec{r}_1 \cdot \hat{r}}}{\pi} e^{in\phi_{scat}}. \tag{23}$$

The scattering from the image of the cylinder can be considered in the same spirit. We thus obtain

$$f^i(\vec{r}, \vec{r}_i) = \sum_{n=-\infty}^{\infty} \frac{-i(-i)^n L B_n e^{-ik\vec{r}_2 \cdot \hat{r}}}{\pi} e^{in\phi_{scat}}. \tag{24}$$

The total scattering function is

$$\begin{aligned} f(\vec{r}, \vec{r}_i) &= \sum_{n=-\infty}^{\infty} \left[\frac{(-i)^{n+1} L A_n e^{-ik\vec{r}_1 \cdot \hat{r}}}{\pi} + \frac{(-i)^{n+1} L B_n e^{-ik\vec{r}_2 \cdot \hat{r}}}{\pi} \right] e^{in\phi_{scat}} \\ &= \sum_{n=-\infty}^{\infty} \left(A_n e^{-ik\vec{r}_1 \cdot \hat{r}} + B_n e^{-ik\vec{r}_2 \cdot \hat{r}} \right) \frac{(-i)^{n+1} L e^{in\phi_{scat}}}{\pi}. \end{aligned} \tag{25}$$

The *reduced* differential scattering cross section is

$$\sigma(\vec{r}, \vec{r}_i) = |f(\vec{r}, \vec{r}_i)/L|^2. \tag{26}$$

The reduced target strength is evaluated from

$$\mathrm{TS} = 10\log_{10}(\sigma). \tag{27}$$

This equation bears much similarity with the scattering strength for the infinite cylinder given in Eq. (13). In the following section, we should compute the target strength for finite cylinders near a pressure release boundary. In particularly, we are interested in the situation of backscattering, in which the scattering direction is opposite to the incident direction, i. e. $\vec{r} = -\vec{r}_i$.

II. NUMERICAL RESULTS

Some interesting properties are found for acoustic scattering by a cylindrical object beneath a flat pressure release plane. Two kinds of cylinders are considered: air-filled and rigid cylinders.

Let us first consider the sound scattering by an air-filled cylinder of length L. Although the theory developed in the last section allows the study of scattering for arbitrary incident and scattering angles, we will first concentrate on backscattering. In addition, without notification we will consider the incident at an angle of $\pi/4$ with respect to the normal to the flat surface. Fig. 2 shows the reduced backscattering target strength in an arbitrary unit as a function of frequency in terms of the non-dimensional parameter ka. The cylinder is placed at the depths of $d/a = 1, 2, 4, 8$, and 16 respectively. For comparison, the situation that the boundary is absent is also plotted. Without boundary, the scattering by a single cylinder has a resonant peak at about $ka = 0.005$. When a flat pressure-plane is added, the scattering from the cylinder will be greatly suppressed for most frequencies under consideration, except for the resonance. At the resonance, the scattering is in fact enhanced by the presence of the surface. This is a unique feature for the cylinder situation. Another effect of the boundary is to shift the resonance peak of the cylinder towards higher frequencies. As the distance between the cylinder and the surface is decreased, the position of the peak moves further towards higher frequencies, and the resonance peak is becoming narrower and narrower. Before the resonance peak, there is a prominent dip in the scattering strength. For the extreme case that the cylinder touches the boundary, the significant dip appears immediately before the resonance. This dip is not observed in the case of a spherical bubble beneath a boundary[7].

When the distance between the cylinder and the surface is increased, the resonance peak moves to lower frequencies until reaching that of the cylinder without a boundary. In Fig. 3, the reduced target strength is plotted against ka for $d/a = 25, 50$, and 100. Here we see that, as the cylinder is moved further from the surface, regular oscillatory features appear in the scattering strength around the values without the boundary. The observed peaks and nulls are mainly due to interference effects between the cylinder and the boundary, as these oscillatory features persist even when the multiple scattering is turned off. The nulls, appearing at some frequency intervals, are more numerous and are spaced more closely together as the cylinder is moved away from the boundary. The peak and null structures are somewhat in accordance with the Lloyd's mirror effect. These features are in analogy with the results shown for the case of a spherical bubble beneath the boundary [7]. However, there is a distinct difference. Namely, the separation between the peaks or between the nulls decreases as the frequency increases.

We have also studied the contributions from different oscillation modes of a cylinder to the scattering. From Eq. (27), it is clear that the scattering is contributed from various vibration modes and the contributions are represented by the summation in which the index n denotes the modes. We find that when the cylinder is located far enough from the surface, the scattering is dominated by $n = 0$ mode for low frequencies (e. g. $ka < 1$); mode $n = 0$ is the omni-directional pulsating mode of the cylinder, i. e. its scattering is uniform in every direction. When the cylinder is moved close to the surface, higher vibration modes become important. These properties are illustrated in Fig. 4. For the extreme case that the cylinder touches the boundary as shown in Fig. 4(a), the result from including only $n = 0$ mode is compared with that including all modes. It is interesting to see that the effect of coupling the pulsating mode with other modes is only to shift the resonance and dip peaks. For low frequencies away from the resonance and the dip, the effect from higher models is not evident. As the cylinder is move away from the surface, the effect of higher modes gradually decreases. For the case $d/a = 4$, the effect of higher modes (i. e. $|n| \geq 2$) virtually diminished.

The effects of the incident angle on the back scattering is shown by Fig. 5. The results show that the scattering is highly anisotropic except at the scattering dip and peak positions; note the scale used in plotting Fig. 5. The fact that the scattering dip does not rely on the incident angle implies that it is not caused by the Lloyd mirror effect. This is because if it were due to the Lloyd mirror effect, different incident angles would lead to different acoustic paths in reflection and incidence and thus result in different phases, causing the scattering pattern to vary.

Next we consider scattering from a rigid cylinder beneath a pressure release boundary. For the rigid cylinder, in contrast to the air cylinder case, the scattering is not so significantly reduced by the presence

of the surface. Instead, it is interesting that the presence of the surface in fact can enhance the scattering strength for most frequencies, except for the frequencies at which the Lloyd effect comes into function. This enhancement is particularly obvious in the low frequency regime. Similar to the air cylinder case, when the distance is large enough, the Lloyd mirror effect causes the scattering strength to oscillate around the values without the boundary for low frequencies. Fig. 6 shows that for low frequencies, the frequency dependence of the scattering is similar for different distances between the cylinder and the surface. For high frequencies, e. g. $ka > 0.4$, the multiple scattering is evident and is shown to increase the scattering strength.

The backscattering by the rigid cylinder under the boundary is anisotropic. This is illustrated in Fig. 7, which shows the backscattering target strength as a function of ka for different incidence angles. The separation between he cylinder and the surface is $d/a = 4$, and the incidence angle is measured with respect to the x-axis, referring to Fig. 1. For low frequencies, i. e. $ka < 0.1$, the scattering is strongest when the incidence is normal to the surface (i. e. for the zero degree incidence). Different from the above air cylinder case, the dips in the scattering strength depend on the incident angles.

Finally we consider the bistatic scattering. The scattering is in the $x - y$ plane (See Fig. 1). We fix the incident angle at 45 degree with respect to the normal to the boundary. The scattering azimuthal angle is measured from the negative direction of the x-axis (Referring to Fig. 1). Fig. 8 shows the scattering angle dependence of the bistatic scattering target strength for the air filled and rigid cylinders respectively. It is interesting to see that when the frequency is low, the scattering tends to be symmetric around the normal to the boundary, i. e. the zero degree scattering angle, for both the air-filled and rigid cylinders. The scattering is strongest at the zero scattering angles. This result indicates that when the frequency is low, the scattering from a cylinder near a boundary bears similar properties of the acoustic radiation from a dipole source, independent of the incident angle. This feature seems against the intuition at the first sight, but can be understood as follows. The scattering from a target can be regarded as a second source radiating waves into the space. From, for instance, Eq. (3), we know that the radiated wave consists of the contributions from all vibration modes of the cylinder. The mode of $n = 0$ is the monopole which radiates an omni-directional wave. At low frequencies, this monopole radiation dominates. In the low frequency regime, both the cylinder and its image radiate waves but in the opposite phase. If the monopole mode dominates, the resulting radiation should appear as that from a dipole source: the strongest radiation is along the dipole axis. This is in fact exactly what is shown by Fig. 8. Comparing Figs. 5 with 7, however, the fact that the bacskscattering relies on the incident angle indicates that the overall bistatic scattering does depend on the incident angle. When the frequency is increased to a certain extent, the bistatic scattering pattern is no longer symmetric around the normal to the boundary.

III. SUMMARY

In this paper, we considered acoustic scattering by cylinders near a pressure-release boundary. A novel method has been developed to describe the multiple scattering between the boundary and the cylinder in terms of an infinite modal series. The complete solution has been derived. Although the theory developed allows for study of various cylinders, for brevity only the cases of air-filled and rigid cylinders are considered. The numerical results show that the presence of the boundary modifies the scattering strength in various ways. One of the most significant discoveries is that the present of the surface can greatly suppress the scattering from 'soft' targets while may enhance rigid bodies. In addition, comparison has been made with the previously investigated case of a spherical air-bubble beneath a pressure-release boundary. The study presented here may link to various applications such as acoustic scattering from ocean-surface dwelling fish or from any underwater elongated objects including submarine.

ACKNOWLEDGEMENT

The work received support from the National Science Council.

References

[1] M. Strasburg, "The pulsating frequency of non-spherical gas bubbles in liquids", J. Acoust. Soc. Am. **25**, 536-537 (1953).

[2] H. N. Oguz and A. Prosperetti, "Bubble oscillation in the vicility of a nearly plane surface", J. Acoust. Soc. Am. **87**, 2085-2092 (1990).

[3] I. Tolstoy, "Superresonant systems of scatterers I.", J. Acoust. Soc. Am. **80**, 282-294 (1986).

[4] G. C. Gaunaurd and H. Huang, "Acoustic scattering by an air-bubble near the sea surface", IEEE J. Ocean. Eng. **20**, 285-292 (1995).

[5] M. Strasburg, "Comments on 'Acoustic scattering by an air-bubble near the sea surface'," IEEE J. Ocean. Eng. **21**, 233 (1996).

[6] G. C. Gaunaurd and H. Huang, "Reply to "Comments on 'Acoustic scattering by an air-bubble near the sea surface'," ", IEEE J. Ocean. Eng. **21**, 233 (1996).

[7] Z. Ye and C. Feuillade, "Sound scattering by an air bubble near a plane sea surface", J. Acoust. Soc. Am. **102**, 789-805 (1997).

[8] Z. Ye, "A novel approach to sound scattering by cylinders of finite length", J. Acoust. Soc. Am. **102**, 877-884 (1997).

[9] L. M. Brekhovskikh, *Waves in Layered Media*, (Academic, New York, 1980).

[10] Z. Ye, E. Hoskinson, R. Dewey, L. Ding, and D. M. Farmer, "A method for acoustic scattering by slender bodies. I. Theory and verification", J. Acoust. Soc. Am. **102**, 1964-1976 (1997).

[11] L. Ding and Z. Ye, "A method for acoustic scattering by slender bodies. II. Comparison with laboratory measurements", J. Acoust. Soc. Am. **102**, 1977-1981 (1997).

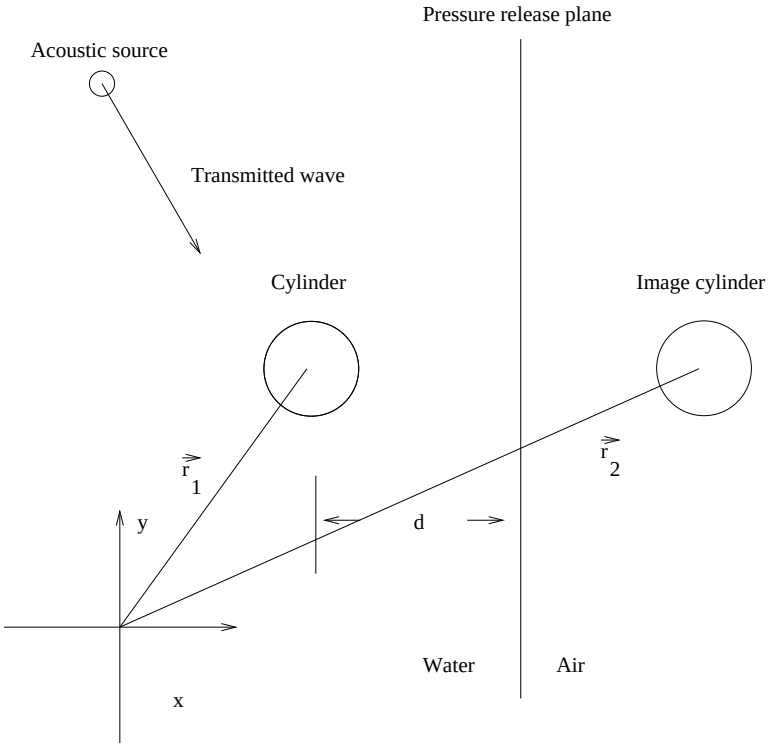

Figure 1: Schematic diagram for an cylinder near a flat pressure release surface

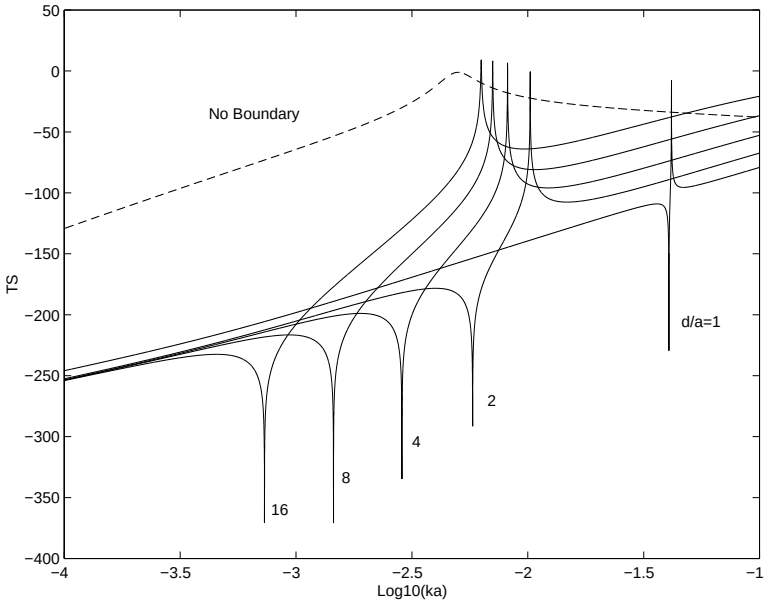

Figure 2: Air Cylinder: Backscattering target strength versus frequency for various d/a values. The incident angle is $\pi/4$.

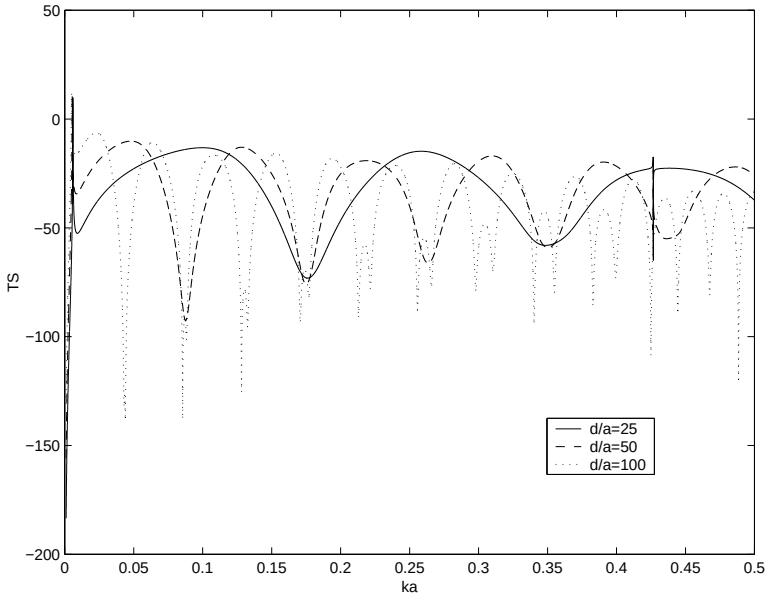

Figure 3: Air Cylinder: Backscattering target strength versus frequency for larger d/a values. The incident angle is $\pi/4$.

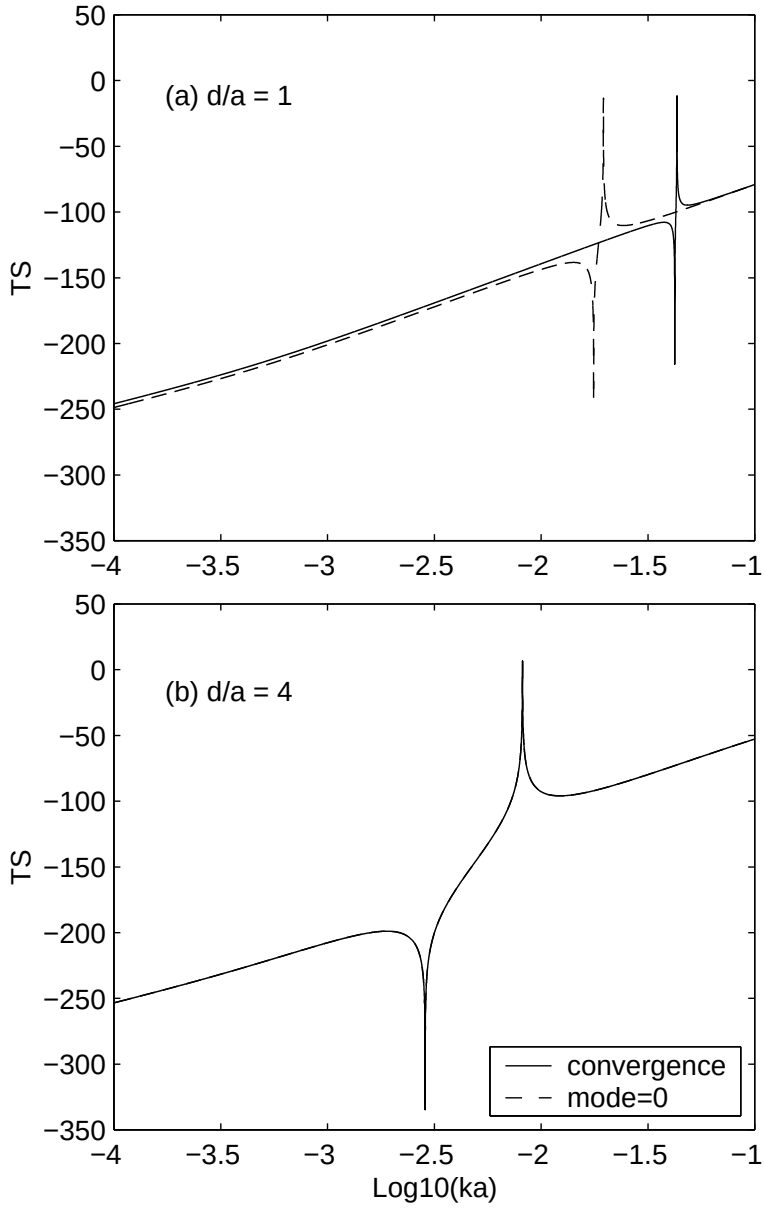

Figure 4: Air Cylinder: Backscattering target strength versus frequency for different modes. The incident angle is $\pi/4$.

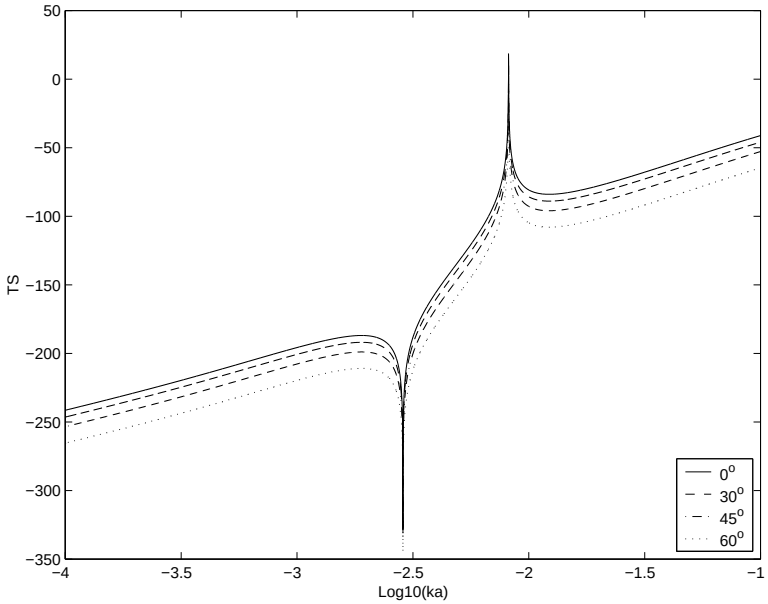

Figure 5: Air Cylinder: Backscattering target strength versus frequency for various incident angles. The incidence angle is measured with respect to the x-axis, referring to Fig. 1. Here $d/a = 4$.

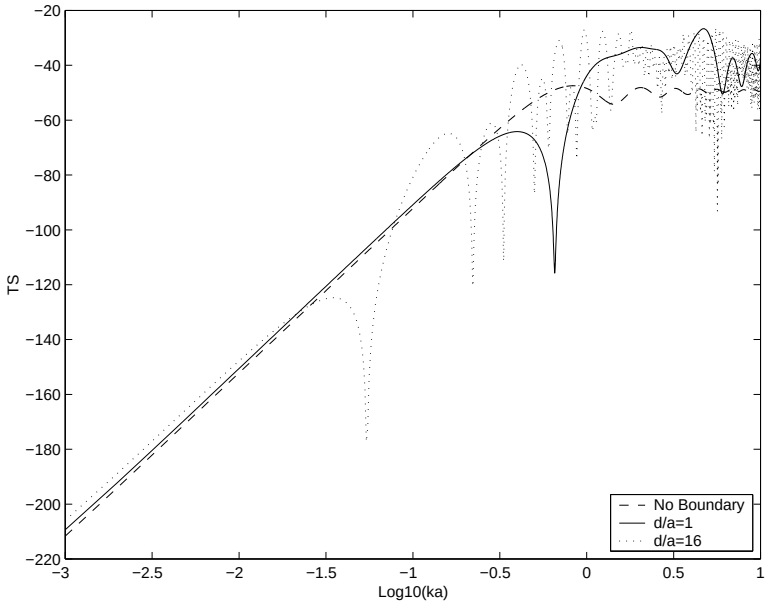

Figure 6: Rigid cylinder: Backscattering target strength versus frequency for various d/a. The incident angle is $\pi/4$.

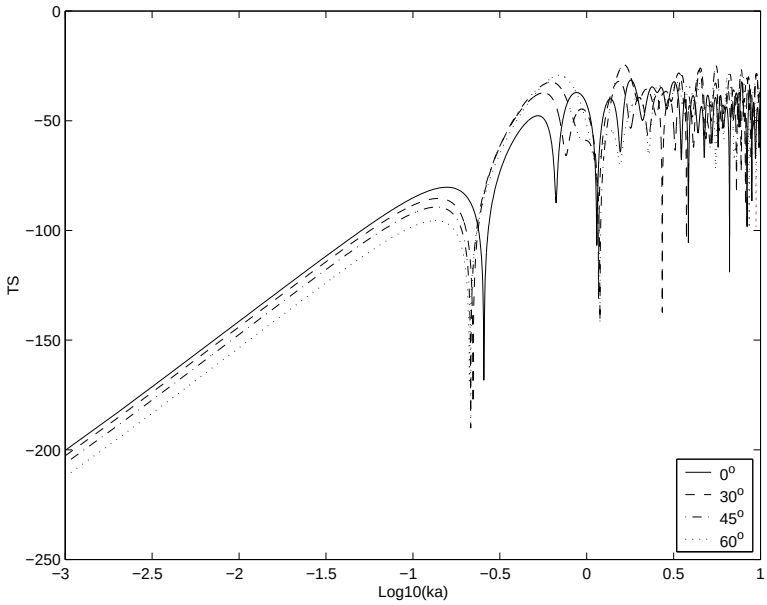

Figure 7: Rigid cylinder: Backscattering target strength versus frequency for various incident angles with $d/a = 4$.

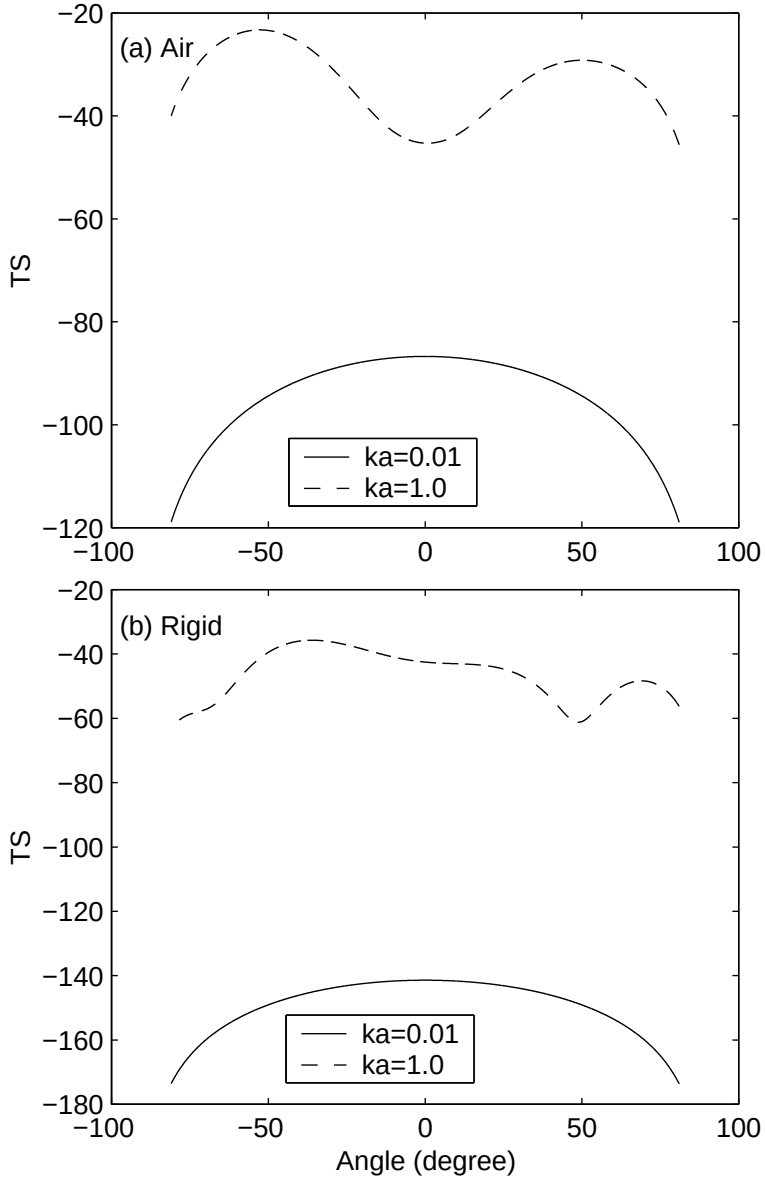

Figure 8: Bistatic scattering target strength versus scattering angle for two frequencies $ka = 0.01, 0.1$: (a) Air-filled cylinder, (b) Rigid cylinder. Here $d/a = 4$ and the incidence angle is 45 degree. The scattering angle is measured with respect to the negative x-axis referring to Fig. 1